NASA Technical Paper 1059

Friction and Wear of Single-Crystal and Polycrystalline Manganese-Zinc Ferrite in Contact With Various Metals

Kazuhisa Miyoshi and Donald H. Buckley

OCTOBER 1977

NASA

NASA Technical Paper 1059

Friction and Wear of Single-Crystal and Polycrystalline Manganese-Zinc Ferrite in Contact With Various Metals

Kazuhisa Miyoshi
Kanazawa University
Kanazawa, Japan
and
Donald H. Buckley
Lewis Research Center
Cleveland, Ohio

NASA
National Aeronautics
and Space Administration
Scientific and Technical Information Office
1977

FRICTION AND WEAR OF SINGLE-CRYSTAL AND POLYCRYSTALLINE MANGANESE-ZINC FERRITE IN CONTACT WITH VARIOUS METALS

by Kazuhisa Miyoshi* and Donald H. Buckley

Lewis Research Center

SUMMARY

An investigation was conducted into the friction and wear behavior of single-crystal (SCF) and hot-pressed polycrystalline (HPF) manganese-zinc ferrite in contact with various metals. Also examined was the nature of interfacial transfer and embedding in the metal of manganese-zinc ferrite. Sliding friction experiments were conducted with SCF and HPF in sliding contact with various metals. All experiments were conducted with light loads of 5 to 50 grams, at a sliding velocity of 3 mm/min, in a vacuum of 10^{-8} N/m^2 and in argon at atmospheric pressure.

The results of the investigation indicate that the coefficients of friction for SCF and HPF in contact with various metals are related to the chemical activity of those metals in a high vacuum. The more active the metal, the higher the coefficient of friction. The more active the metal, the lower the load at which stick-slip behavior is observed. The coefficients of friction for both SCF and HPF in contact with metals were the same and much higher in vacuum than in argon at atmospheric pressure. All the metals tested transferred to the surfaces of both SCF and HPF in sliding. Both SCF and HPF exhibited cracking and fracture with sliding. Cracking in SCF is dependent on crystallographic characteristics. In HPF, cracking is a function of the orientation of the individual crystallites. The cracks generally begin in a grain boundary and extend along it. Further, the wear debris may be transferred to the metals. The wear debris of SCF and HPF, produced in sliding, rolls and slides on both the metal and manganese-zinc ferrite surfaces and produces rows of indentations and deep grooves on these surfaces.

---

* Assistant Professor of Precision Engineering, Kanazawa University, Kanazawa, Japan; National Research Council - National Aeronautics and Space Administration Research Associate.

INTRODUCTION

The magnetic characteristics of ceramic materials are of increasing importance as the field of solid-state electronics continues to expand. Ceramic magnets are often used in high-frequency devices in which the greater resistivity of the ferrimagnetic oxide gives them a decisive advantage over metals. They have found use, for example, as circuit elements for television and magnetic recording devices (e.g., video tape recorders). The use of ceramic magnets as memory units with rapid switching times in digital computers has been essential to the explosion of computer technology (ref. 1). Further, magnetic ceramics (e.g., manganese-zinc ferrite) are becoming increasingly important as circuit elements in electronic devices that are required to have desirable wear resistance and low friction behavior (refs. 2 to 4).

The friction and wear properties of magnetic ceramic materials in contact with metals and ceramics under a variety of exacting environmental conditions are, however, not fully understood. Very little experimental work has been done, for example, with manganese-zinc ferrite, a commonly used magnetic ceramic (ref. 5). Fundamental studies on the friction and wear behavior of magnetic ceramic materials in contact with metals and ceramics should commence with clean surfaces. Such surfaces can be obtained and maintained in a vacuum environment. Once the behavior of clean surfaces is understood, the effect of environmental constituents on friction and wear can be identified. Thus, the friction and wear behavior of magnetic ceramic materials in high vacuum is important. In addition, the knowledge gained in such studies may assist in achieving a better understanding of the friction and wear properties of brittle materials.

The object of the present investigation was to examine the friction and wear behavior of single-crystal and polycrystalline manganese-zinc ferrite in contact with various metals and to examine the nature of interfacial transfer and embedding in the metal of manganese-zinc ferrite. All experiments were conducted with light loads of 5 to 50 grams, at a sliding velocity of 3 mm/min, both in a high vacuum of 10^{-8} N/m^2 and in argon at atmospheric pressure. Studies were all at room temperature.

MATERIALS

The single-crystal manganese-zinc ferrite (SCF) as-grown platelets used in these experiments were 99.9-percent-pure oxide, as shown in table I. The hot-pressed polycrystalline manganese-zinc ferrite (HPF) was also 99.9-percent-pure oxide. The porosity of polycrystalline manganese-zinc ferrite is less than 0.1 percent.

The ferrimagnetic oxides known as ferrites have the general formula $M^{2+}O \cdot Fe_2^{3+}O_3$, where M^{2+} is a divalent metallic ion such as Mn^{2+}, Zn^{2+}, Fe^{2+}, Ni^{2+}, Cu^{2+}, or Mg^{2+}. Mixed ferrites $M_{1-x}Zn_xFe_2O_4$, where M is a divalent ion, can also be

fabricated. In these compositions the divalent cation may be a mixture of ions (e.g., $Mn_{1-x}Zn_xFe_2O_4$), so that a wide range of compositions and magnetic properties is possible. The crystal structure is that of the spinels in which the oxygen ions are in a nearly close-packed cubic array. In a unit cell, which contains 32 oxygen ions, there are 32 octahedral sites and 64 tetrahedral sites; of these, 16 of the octahedral sites and 8 of the tetrahedral sites are filled. All the ferrimagnetic spinels are more or less inverse spinel; that is, the 8 tetrahedral sites are filled with trivalent ions and the 16 octahedral sites are equally divided between divalent and trivalent ions.

The single-crystal manganese-zinc ferrite had the (110) surface parallel to the sliding interface and the (001) surface perpendicular to the sliding direction. The {110} planes in the ⟨001⟩ directions exhibit the greatest hardness in ferrite (table I). The method of determining the orientation of the single crystal is the back-reflection Laue method.

All of the metals were polycrystalline. The titanium was 99.97 percent pure, the copper was 99.999 percent pure, and all the other metals were 99.99 percent pure (table II).

APPARATUS

Two apparatuses were used in this investigation. One was a vacuum system capable of measuring adhesion, load, and friction. The apparatus also contained tools for surface analysis, an Auger emission spectrometer, and a LEED (low-energy electron diffraction system). The mechanism used for measuring adhesion, load, and friction is shown schematically in figure 1(a). A gimbal-mounted beam is projected into the vacuum system. The beam contains two flats machined normal to each other with strain gages mounted thereon. The end of the rod contains the metal pin specimen. As the beam is moved normal to the disk, a load is applied that is measured by the strain gage. The vertical sliding motion of the pin along the disk surface is accomplished through a motorized gimbal assembly. Under an applied load, the friction force is sensed by the strain gage normal to that used to measure load. Multiple wear tracks could be generated on the disk specimen surface by translational motion of the beam containing the pin. This feature was used to examine the coefficient of friction at various loads. Pin sliding was in the vertical direction, as shown in figure 1(a). The vacuum apparatus in which the components of figure 1(a) were contained also had a LEED system and an Auger spectrometer. The electron beam from both LEED and Auger spectroscopy could be focused on any disk site desired. The disk specimen was always manganese-zinc ferrite. The pins were various metals.

The second apparatus was a system capable of measuring friction in argon. The mechanism for measuring friction is shown schematically in figure 1(b). The beam

contains one flat machined normal to the direction of friction application. The end of the rod contains the metal pin specimen. The load is applied by placing deadweights on a pan that sets on top of the rod. Under an applied load the friction force is sensed by a strain gage.

EXPERIMENTAL PROCEDURE

The disk flat specimens were polished with a diamond powder, and the metal pin specimens were also polished with an aluminum oxide (Al_2O_3) powder. Both powders had particle diameters of 1 micrometer. The radius of the pin specimens was 0.79 millimeter. The surfaces of the disk and pin specimens were rinsed with 200-proof ethyl alcohol.

For the experiments in vacuum the specimens were placed in the vacuum chamber and the system was evacuated and subsequently baked out to achieve a pressure of 1.33×10^{-8} N/m^2 (10^{-10} torr). When this pressure was achieved, argon gas was bled back into the vacuum chamber to a pressure of 1.3 N/m^2. A 1000-volt, direct-current potential was applied and the specimens (both disk and rider) were argon sputter bombarded for 30 minutes. After 1 hour the vacuum chamber was reevacuated and Auger spectra of the disk surface were obtained to determine the degree of surface cleanliness. When the disk surface was clean, friction experiments were conducted.

Loads of 5 to 50 grams were applied to the pin-disk contact by deflecting the beam of figure 1(a). Both load and friction force were continuously monitored during a friction experiment. Sliding velocity was 3 mm/min, with a total sliding distance of 3 millimeters. All friction experiments in vacuum were conducted with the system reevacuated to a pressure of 10^{-8} N/m^2. All friction experiments at atmospheric pressure were conducted with the system in argon.

RESULTS AND DISCUSSION

Auger Analysis of Manganese-Zinc Ferrite Surfaces

An Auger emission spectroscopy spectrum of the single-crystal manganese-zinc ferrite surface (SCF) obtained before sputter cleaning is shown in figure 2(a-1). The crystal was in the as-received state after it had been baked out in the vacuum system. In addition to the oxygen and small iron peaks indicated, a carbon contamination peak is evident. An Auger spectrum for the single-crystal manganese-zinc surface obtained after sputter cleaning is shown in figure 2(a-2). The carbon contamination peak has completely disappeared from the spectrum. In addition to the oxygen and iron, Auger peaks

indicate small amounts of manganese and negligibly small amounts of zinc on the surface.

Auger spectra of the as-received hot-pressed polycrystalline manganese-zinc ferrite (HPF) surface were also obtained before and after sputter cleaning. The spectra (fig. 2(b)) are almost the same as those for the SCF surface.

Friction Behavior of Manganese-Zinc Ferrite

Sliding friction experiments were conducted with SCF and HPF in contact with various metals. Data were obtained for clean iron in sliding contact with SCF and HPF surfaces as a function of load. Typical results are presented in figure 3. The difference in friction over the entire load range between SCF-iron and HPF-iron is negligibly small.

Figure 4 shows the coefficients of friction measured at various loads for iron sliding on SCF both in high vacuum and in argon at atmospheric pressure. The marked difference in friction over the entire load range for the two environments shows the effect of oxides and adsorbates on the friction properties of the SCF-metal couple.

The coefficients of friction for various metals sliding on SCF and HPF both in vacuum and in argon at atmospheric pressure were unaffected by load. Figure 5 presents the coefficients of friction. The results in high vacuum are to be anticipated from the chemical interaction and the important role it plays in the friction of SCF (or HPF)-metal couples. This subject is explained in detail in the following section. The coefficients of friction in argon at atmospheric pressure are all approximately 0.1 to 0.2. Thus, the chemical activity or inactivity of a metal does not appear to play a role in the friction of SCF in contact with metals in argon. A prerequisite for this sameness in friction is that the metals form a stable metal oxide. The oxides of the metals in figure 5 are all very stable.

Effect of Metal Activity on Friction

The relative chemical activity of the transition metals (metals with partially filled d shells) as a group can be ascertained from their percent d bond character after Pauling (ref. 6). The friction properties of metals have been shown to be related to this character (ref. 7). The greater the percent of d bond character, the less active is the metal.

The coefficients of friction for a number of transition metals with SCF are presented in figure 6 as a function of the d bond character of the transition metal. There appears to be good agreement between friction and chemical activity of the transition metals. Titanium, having strong chemical affinity for iron and oxygen, exhibits considerably

higher friction in contact with SCF than does rhodium, which has a lesser affinity for these same two elements.

The friction traces with metal-SCF couples under lower loads are characterized by smoothly fluctuating behavior with no evidence of stick-slip (fig. 7(a)). On the other hand, the traces under higher loads are characterized by stick-slip behavior. With the chemically more active metal titanium, more marked stick-slip behavior appears under lower load (about 20 g). With the chemically less active metal rhodium, stick-slip behavior appears under higher load (35 g or more).

Transfer and Wear of Metals Sliding on Manganese-Zinc Ferrite

All SCF and HPF specimens contacted by the metals in figure 6 were found to contain on their surfaces the metal elements, indicating transfer of the metal to the ferrite, as presented by figure 8. Figures 8(a) to (c) are scanning electron micrographs and X-ray dispersive analysis of the HPF surface of the thin films and wear debris of tungsten transferred to HPF. The concentrations of white spots in figure 8(c) correspond to those locations in figure 8(b) where transfer of metallic tungsten has occurred. The copious amounts of transferred tungsten seen in figure 8(a) are a result of a single pass of a tungsten rider over the HPF surface. After the single-pass experiments, multipass experiments were conducted to establish equilibrium friction. When repeated passes were made of the metal rider over the same manganese-zinc ferrite specimen (SCF and HPF), the coefficient of friction was nearly constant, as indicated by the data of figure 9. In figure 9, friction data were obtained for titanium and rhodium sliding on SCF both in vacuum and in argon at atmospheric pressure.

The wear scar on the metal rider after it slid against manganese-zinc ferrite revealed evidence of a large number of plastically deformed grooves (fig. 10) and cracks (figs. 11 and 12). Cracking is explained in detail in the following section. Figure 10 shows scanning electron micrographs of the rider wear scar on titanium resulting from five passes of the titanium rider over the SCF surface in vacuum.

Cracking and Embedding of Manganese-Zinc Ferrite

Detailed examinations of the wear track on a manganese-zinc ferrite surface after sliding with metals revealed evidence of fracture in both SCF (fig. 11) and HPF (fig. 12). Figures 11 and 12 are scanning electron micrographs of wear tracks on SCF and HPF. In figure 11, three types of cracking in the wear track are observed. These appear only occasionally. One type is characterized by a small crack propagating perpendicular to the sliding direction. Later observations show that it propagates below the surface from

the high compressive stress at the real contact area of the rider during sliding. The second type is a crack propagating at an inclination of about 45° to the sliding direction, that is, along cleavage planes of {110}. The third type obtained is a crack propagating parallel to the sliding direction, that is, also along the cleavage planes of {110}.

The three types of cracking were also observed with SCF in sliding contact with diamond in nitrogen at atmospheric pressure (ref. 5) and with single-crystal silicon carbide in sliding contact with diamond in argon at atmospheric pressure (ref. 8). Under such conditions, sliding occurred at the interface and friction primarily involved shearing at the interface and plowing (plastic deformation) in single-crystal silicon carbide.

It is of interest that similar cracking occurs in nominally brittle materials regardless of marked differences in friction behavior and environments. Figure 12, however, reveals that the extent of small cracking in HPF depends on the orientation of the individual crystallites and the direction of sliding. It is obvious that a significant degree of cracking begins in a grain boundary and extends along the HPF grain boundaries. The fracturing of the HPF surface is the result of cracks propagating and intersecting other cracks in grain boundaries. The cracks and fracture can originate from a void (fig. 12(d)); voids are primarily in grain boundaries.

The wear scars on metals after sliding on SCF and HPF surfaces may contain occasional small wear debris generated by the fracture of the SCF and HPF surfaces and their transfer to the metal surfaces, as shown in figure 13. Titanium, having strong chemical activity, exhibits considerably more wear debris of SCF transferred to its surface than do rhodium or iron, which have lesser chemical activity (fig. 14).

Figure 15 reveals that wear debris of SCF and HPF, produced in sliding, plowed both the metal and manganese-zinc ferrite surfaces. This debris rolls and slides on both the metal and manganese-zinc ferrite surfaces (fig. 16) and produces the indentations and deep grooves shown in figure 15. A similar deformation behavior was observed with titanium in sliding contact with single-crystal silicon carbide (ref. 9).

Figure 15 shows straight rows of indentations along the sliding direction formed by rolling of SCF wear debris. The rows of indentations are not unique but are generally observed (fig. 10). Figure 15 also shows grooves along the sliding direction on both the metals (rhodium, cobalt, and nickel) and the manganese-zinc ferrites.

CONCLUSIONS

As a result of the sliding friction experiments conducted in this investigation with single-crystal and polycrystalline manganese-zinc ferrites (SCF and HPF) in sliding contact with various metals, the following conclusions are drawn:

1. The coefficients of friction for SCF and HPF in contact with various metals are related to the relative chemical activity of those metals in a high vacuum (10^{-8} N/m^2).

The more active the metal, the higher the coefficient of friction. The more active the metal, the lower the load at which stick-slip behavior is observed.

2. The coefficients of friction for both SCF and HPF in contact with metals are the same and are much higher in vacuum than in argon at atmospheric pressure.

3. All metals transferred to the surfaces of both SCF and HPF in sliding.

4. The SCF and HPF exhibit cracking and fracture with sliding. Cracking in SCF is dependent on crystallographic characteristics (such as cleavage of {110}). In HPF, cracking depends on the orientation of the individual crystallites. The cracks generally begin in a grain boundary and extend along it. Further, the wear debris may be transferred to the metals.

5. The wear debris of SCF and HPF, produced in sliding, rolls and slides on both the metal and manganese-zinc ferrite surfaces and produces rows of indentations and deep grooves on these surfaces.

Lewis Research Center,
National Aeronautics and Space Administration,
Cleveland, Ohio, July 25, 1977,
506-16.

REFERENCES

1. Kingery, W. D.; Bowen, H. K.; and Uhlmann, D. R.: Introduction to Ceramics. Second ed., John Wiley & Sons, Inc., 1976, pp. 975-1014.

2. Tanaka, K.; et al.: Friction and Wear in the Sliding of VTR Head against Magnetic Tape (1st Report) - Contact Force and Frictional Force. J. Jpn Soc. Precision Eng., vol. 40, no. 7, July, 1974, pp. 550-556.

3. Tanaka, K.; et al.: Friction and Wear in the Sliding of VTR Head against Magnetic Tape (2nd Report) - Wear of VTR Head Made of a Ferrite Single Crystal. J. Jpn. Soc. Precision Eng., vol. 40, no. 8, Aug. 1974, pp. 651-657.

4. Tanaka, K.; et al.: Friction and Wear in the Sliding of VTR Head against Magnetic Tape (3rd Report) - Effect of Wear on the Output Signal Level. J. Jpn. Soc. Precision Eng., vol. 40, no. 9, Sept. 1974, pp. 785-791.

5. Tanaka, K.; et al.: Friction and Deformation of Mn-Zn Ferrite Single Crystals. Proceedings of the JSLE-ASLE International Lubrication Conference, Tokyo, 1975, T. Sakurai, ed., Elsevier Scientific Publishing Co., 1976, pp. 58-66.

6. Pauling, L.: A Resonating-Valence-Bond Theory of Metals and Intermetallic Compounds. Proc. R. Soc., London, Ser. A, vol. 196, no. 1046, Apr. 7, 1949, pp. 362.

7. Buckley, D. H.: The Metal-to-Metal Interface and its Effect on Adhesion and Friction. J. Colloid Interface Sci., vol. 58, no. 1, Jan. 1977, pp. 36-53.

8. Miyoshi, Kazuhisa; and Buckley, Donald H.: Friction and Deformation Behavior of Single-Crystal Silicon Carbide. NASA TP-1053, 1977.

9. Miyoshi, Kazuhisa; and Buckley, Donald H.: Friction and Wear Behavior of Single-Crystal Silicon Carbide in Contact with Titanium. NASA TP-1035, 1977.

TABLE I. - COMPOSITION AND HARDNESS DATA

ON MANGANESE-ZINC FERRITE

(a) Single-crystal Mn-Zn ferrite (SCF)

	Composition, wt %							
	Fe_2O_3, 71.6		MnO, 17.3				ZnO, 11.1	
Surface	(100)	(100)	(110)	(110)	(111)	(111)	(211)	(211)
Direction	[001]	[011]	[001]	$[\bar{1}10]$	$[11\bar{2}]$	$[1\bar{1}0]$	$[\bar{1}11]$	$[0\bar{1}1]$
Knoop hardness[a]	630	560	630	560	580	600	550	580
Vickers hardness[b]	630	630	645	645	590	590	650	650

(b) Hot-pressed polycrystalline Mn-Zn ferrite (HPF)

	Composition, wt %		
	Fe_2O_3, 69.1	MnO, 15.2	ZnO, 15.7
Grain size, μm	24	24	24
Porosity, percent	<0.1	<0.1	<0.1
Vickers hardness[b]	640	640	640

[a]Knoop hardness measuring load was 300 grams.

[b]Vickers hardness measuring load was 50 grams.

TABLE II. - CRYSTAL STRUCTURE AND

PURITY OF VARIOUS METALS

Metal	Crystal structure	Purity, percent
W	Body-centered cubic	99.99
Fe	Body-centered cubic	99.99
Mo	Body-centered cubic	99.99
Cu	Face-centered cubic	99.999
Ni	↓	99.99
Al	↓	99.99
Rh	↓	99.99
Ti	Close-packed hexagonal	99.97
Co	Close-packed hexagonal	99.99
Zn	Close-packed hexagonal	99.99

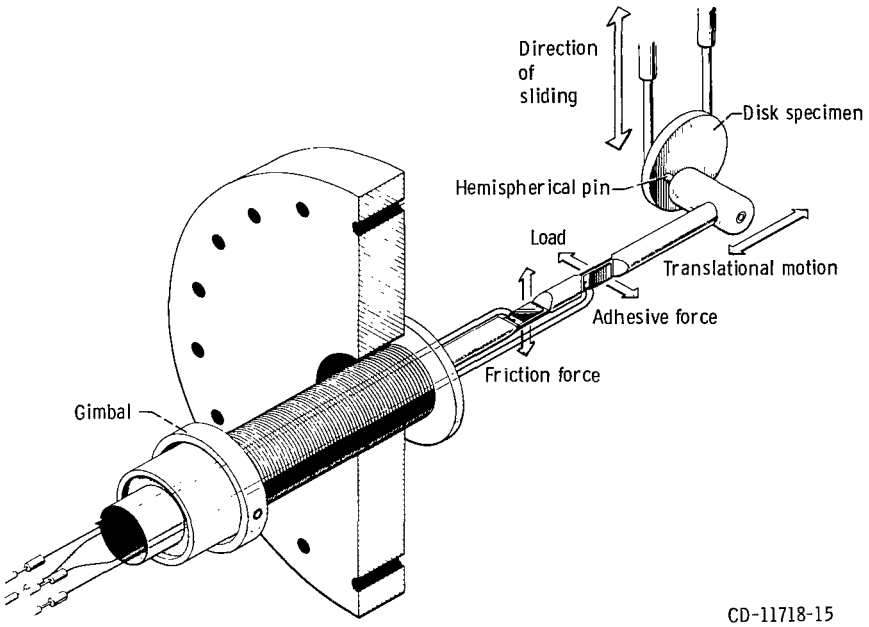

(a) High-vacuum apparatus.

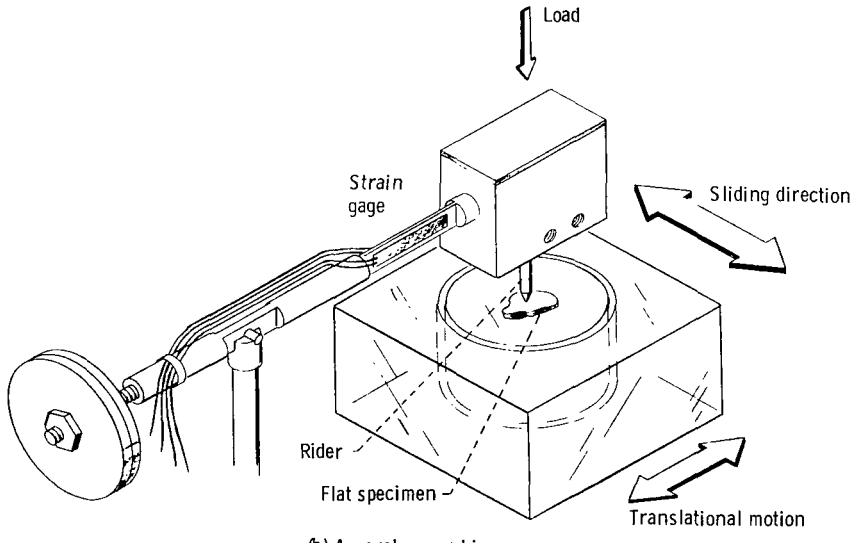

(b) Apparatus used in argon.

Figure 1. - Friction and wear apparatus.

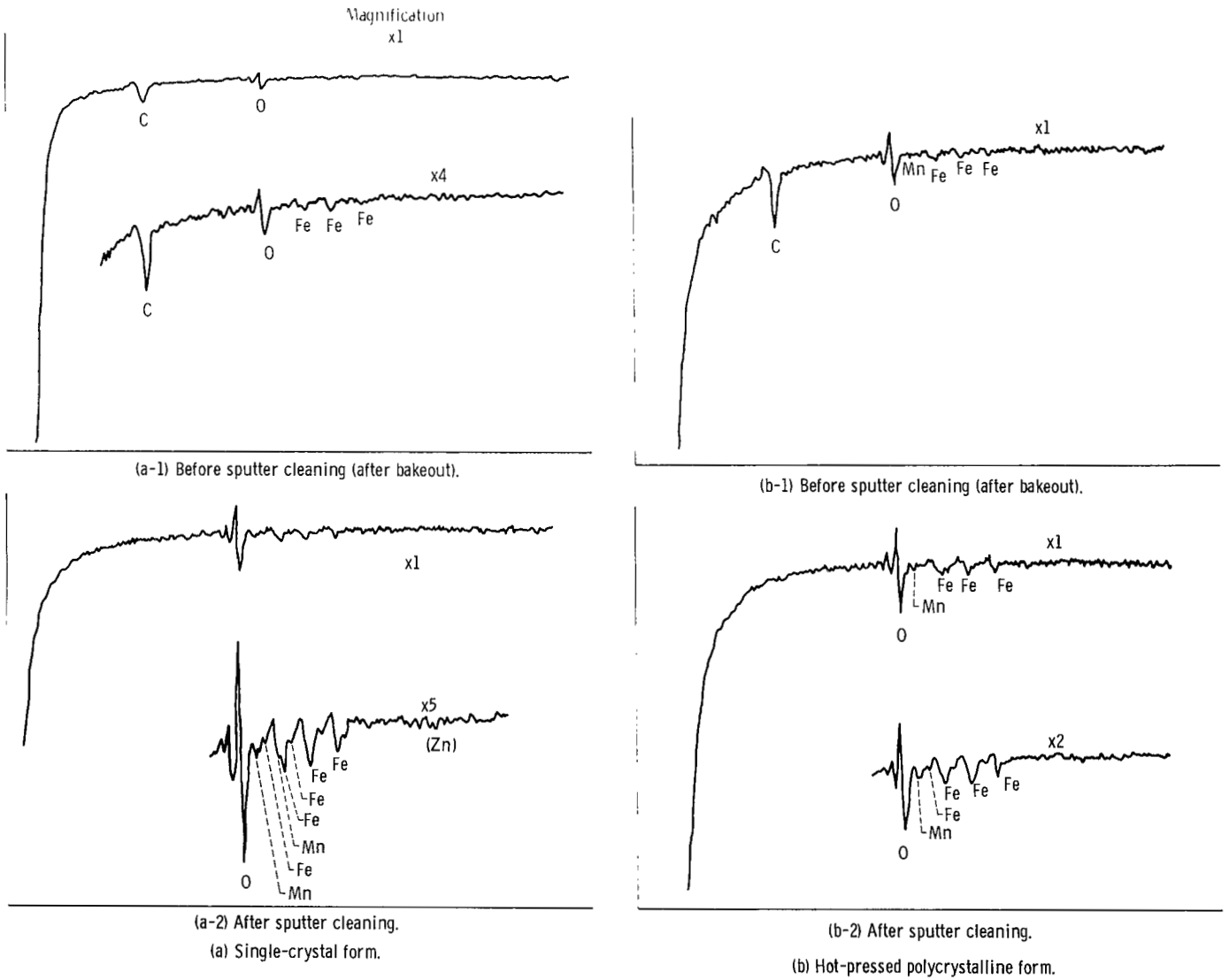

Figure 2. - Auger emission spectroscopy spectra for manganese-zinc ferrite.

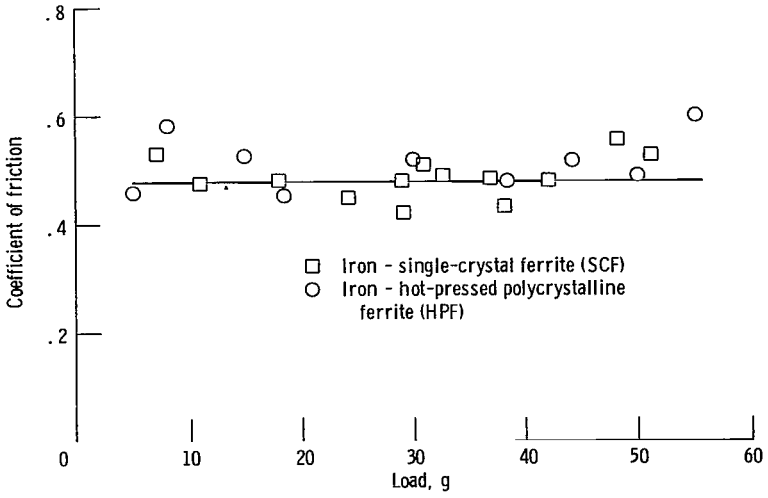

Figure 3. - Coefficient of friction as function of load for single pass of iron rider sliding on single-crystal (110) and hot-pressed polycrystalline manganese-zinc ferrite surfaces in high vacuum (10^{-8} N/m^2). Sliding velocity, 3 mm/min; temperature, 25° C.

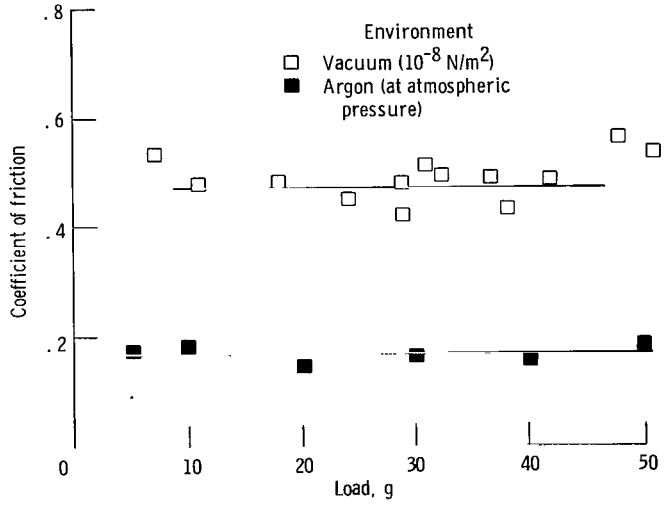

Figure 4. - Coefficient of friction as function of load for single pass of iron rider sliding on single-crystal manganese-zinc ferrite (110) surface both in high vacuum (10^{-8} N/m^2) and in argon at atmospheric pressure. Sliding velocity, 3 mm/min; temperature, 25° C.

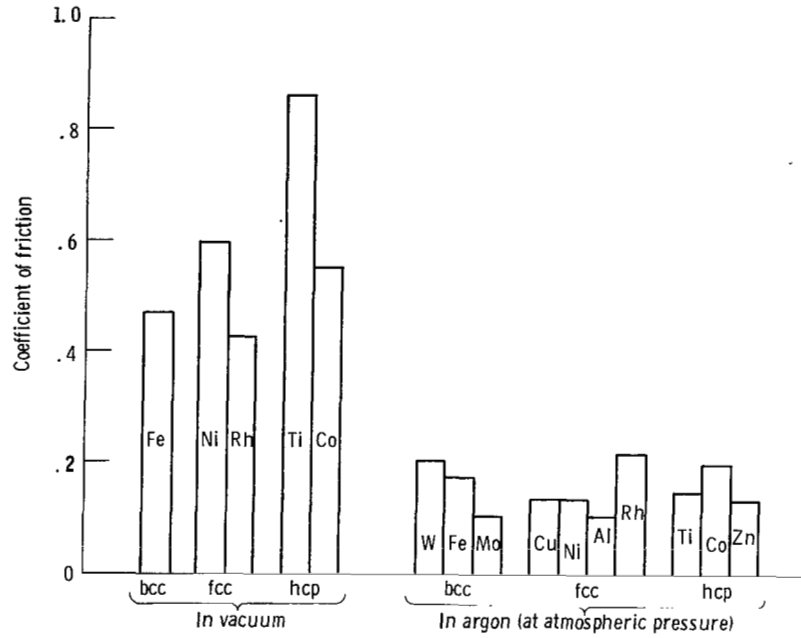

Figure 5. - Coefficient of friction for single passes of various metal riders sliding on single-crystal manganese-zinc ferrite (110) surface both in high vacuum (10^{-8} N/m^2) and in argon at atmospheric pressure. Sliding velocity, 3 mm/min; load, 5 to 50 grams; temperature, 25^0 C.

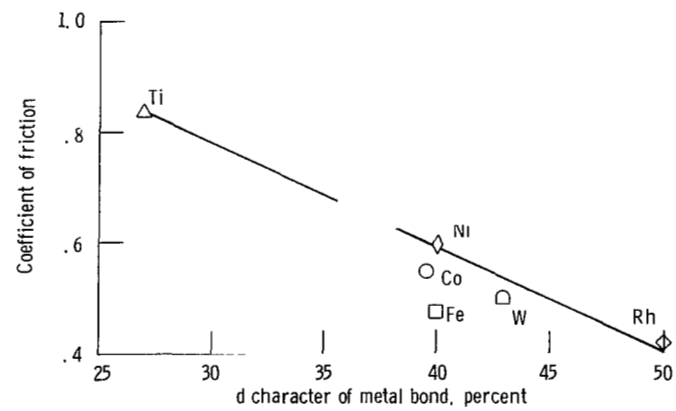

Figure 6. - Coefficient of friction as function of percent of d bond character of various metals in sliding contact with single-crystal manganese-zinc ferrite (110) surface in vacuum (10^{-8} N/m^2). Single pass; sliding velocity, 3 mm/min; load, 30 grams; temperature, 25^0 C.

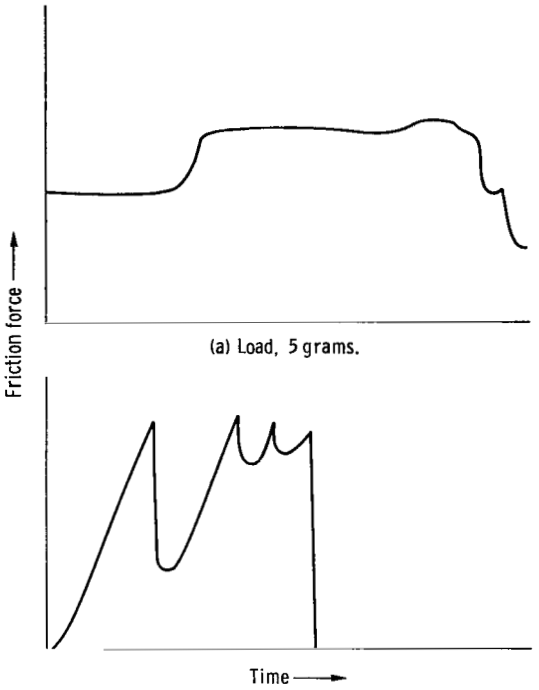

(a) Load, 5 grams.

(b) Load, 26 grams.

Figure 7. - Friction traces in vacuum (10^{-8} N/m^2) for single pass of titanium rider sliding on single-crystal manganese-zinc ferrite surfaces. Sliding velocity, 3 mm/min; temperature, 25^0 C.

(a) Wear track.

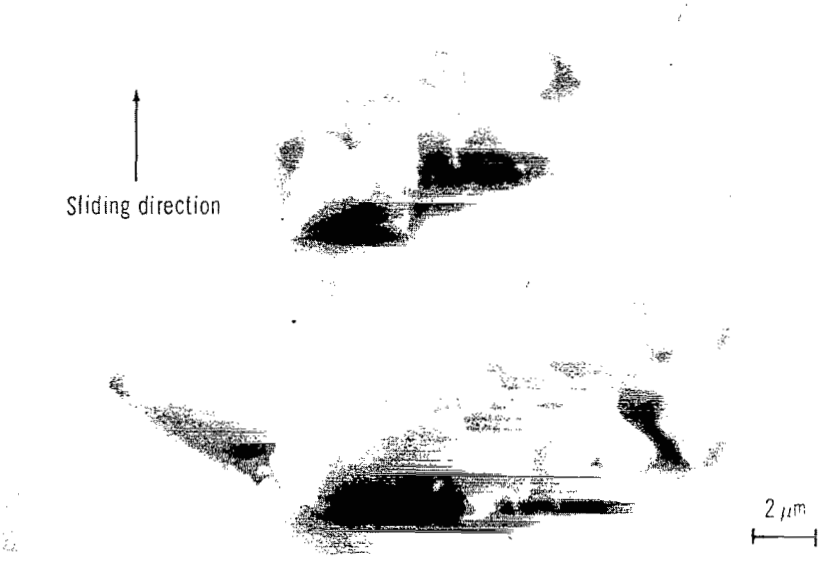

(b) Thin film and wear debris of tungsten transferred to HPF.

Figure 8. - Scanning electron micrographs and energy dispersive X-ray analysis of wear track on hot-pressed polycrystalline manganese-zinc ferrite surface as result of single pass of tungsten rider in high vacuum (10^{-8} N/m^2). Sliding velocity, 3 mm/min; load, 50 grams; temperature, 25° C.

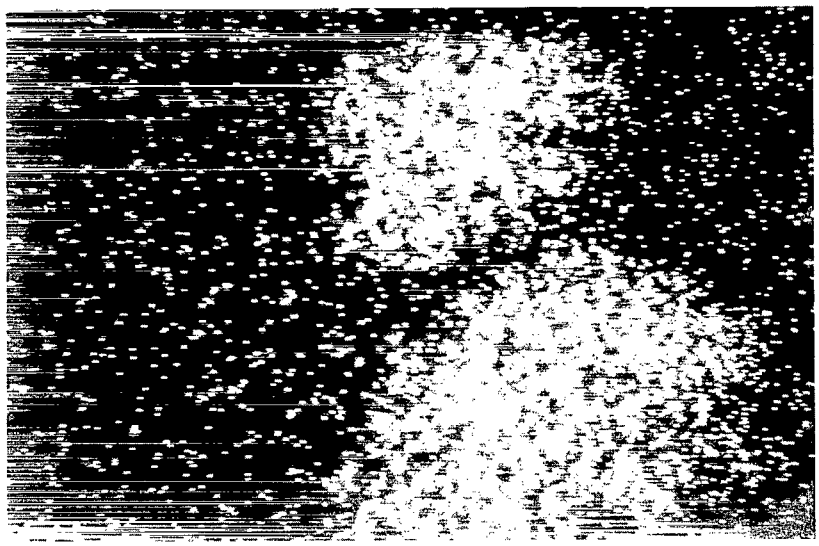

(c) Tungsten K_α X-ray map of HPF; 8×10^3 counts.

Figure 8. - Concluded.

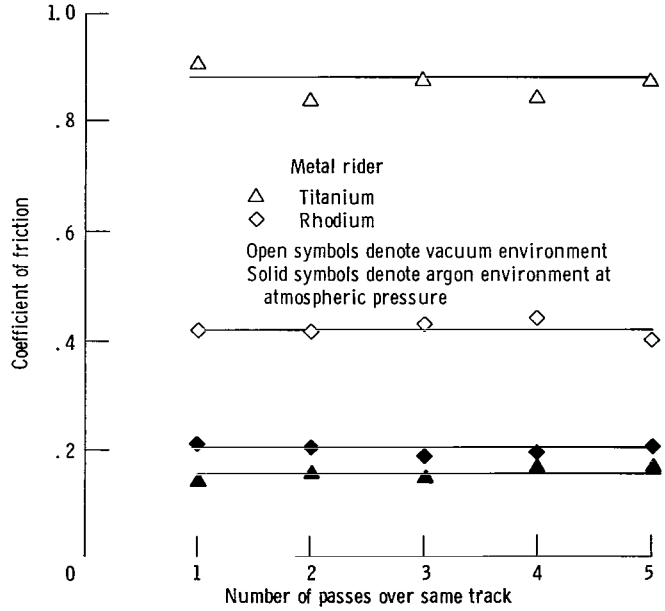

Figure 9. - Coefficient of friction as function of number of passes of metal rider across single-crystal manganese-zinc ferrite (110) surface, both in high vacuum (10^{-8} N/m^2) and in argon at atmospheric pressure. Sliding velocity, 3 mm/min; load, 30 grams; temperature, 25^0 C.

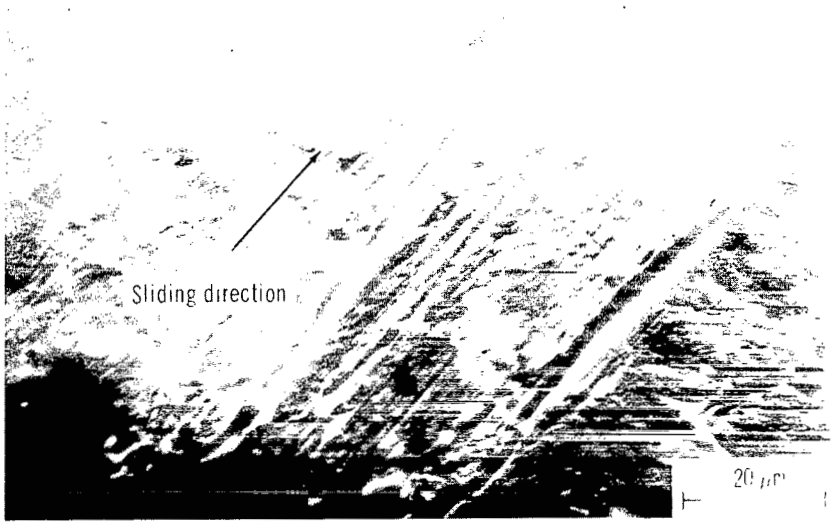

(a) Wear scar as result of five passes.

(b) Plastically deformed grooves.

Figure 10. - Scanning electron micrographs of wear scar on titanium rider after sliding on single-crystal manganese-zinc ferrite (110) surface in high vacuum (10^{-8} N/m^2). Sliding velocity, 3 mm/min; load, 30 grams; temperature, 25° C.

(a) Cracks propagating perpendicular to, parallel to, and at an inclination of about 45° to sliding direction.

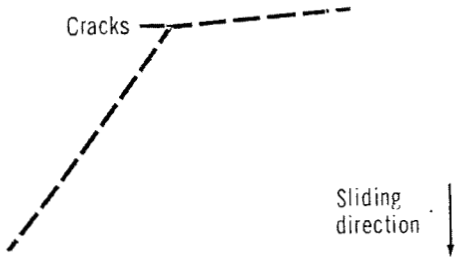

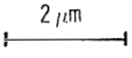

(b) Cracks propagating perpendicular to and at an inclination of 45° to sliding direction.

Figure 11. - Scanning electron micrographs of wear track and cracking of single-crystal manganese-zinc ferrite (110) surface after five passes of cobalt rider in high vacuum (10^{-8} N/m^2). Sliding velocity, 3 mm/min; temperature, 25° C.

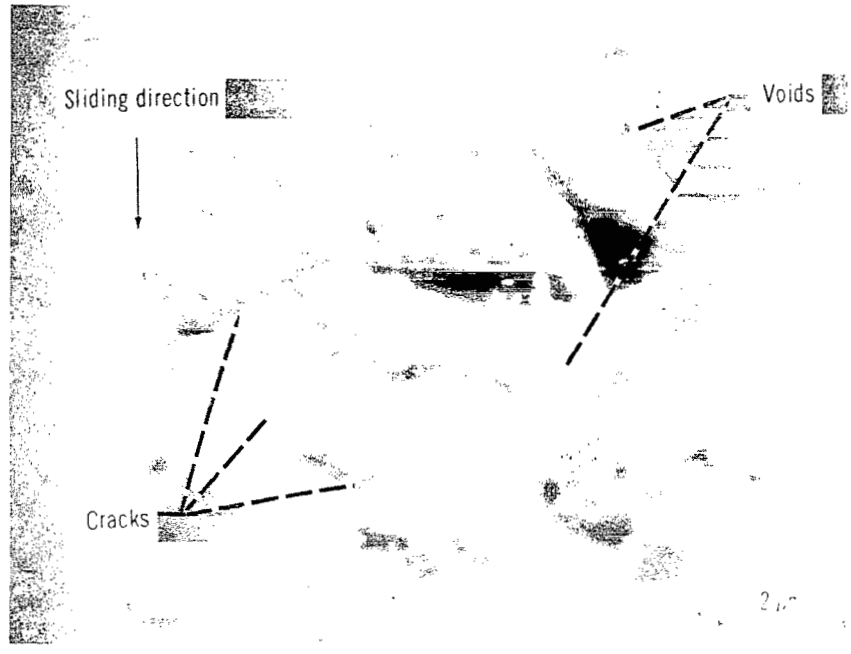

(a) Cracking around grain.

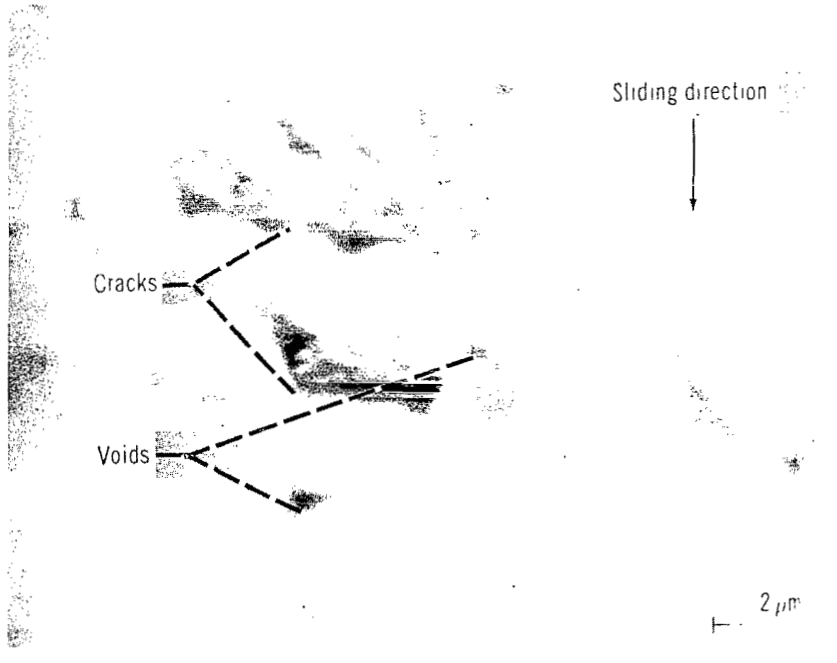

(b) Cracks propagating nearly perpendicular to sliding direction.

Figure 12. - Scanning electron micrographs of wear track and cracking of hot-pressed polycrystalline manganese-zinc ferrite surface (etched) after five passes of rhodium rider in high vacuum (10^{-8} N/m^2). Sliding velocity, 3 mm/min; temperature, 25° C.

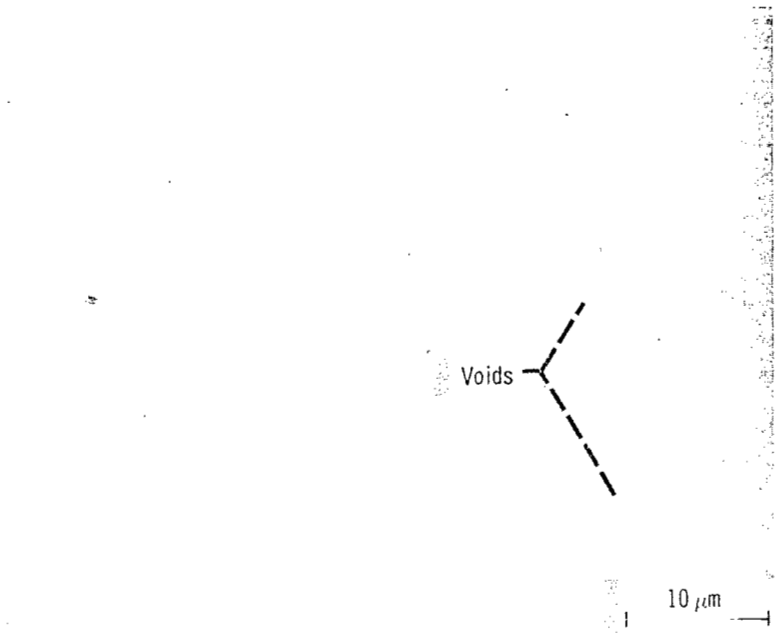

(c) Microstructure of HPF (etched) before sliding of rhodium rider.

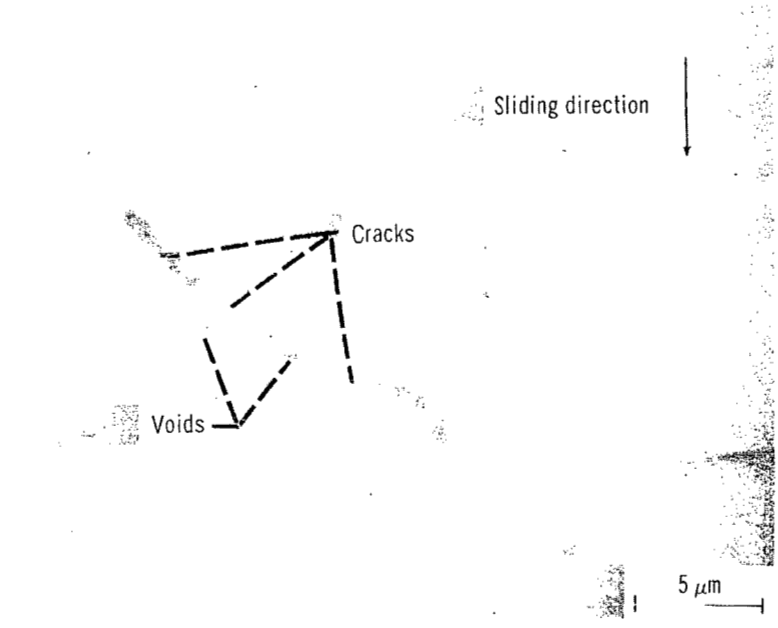

(d) Cracks propagating along grain boundary.

Figure 12. - Concluded.

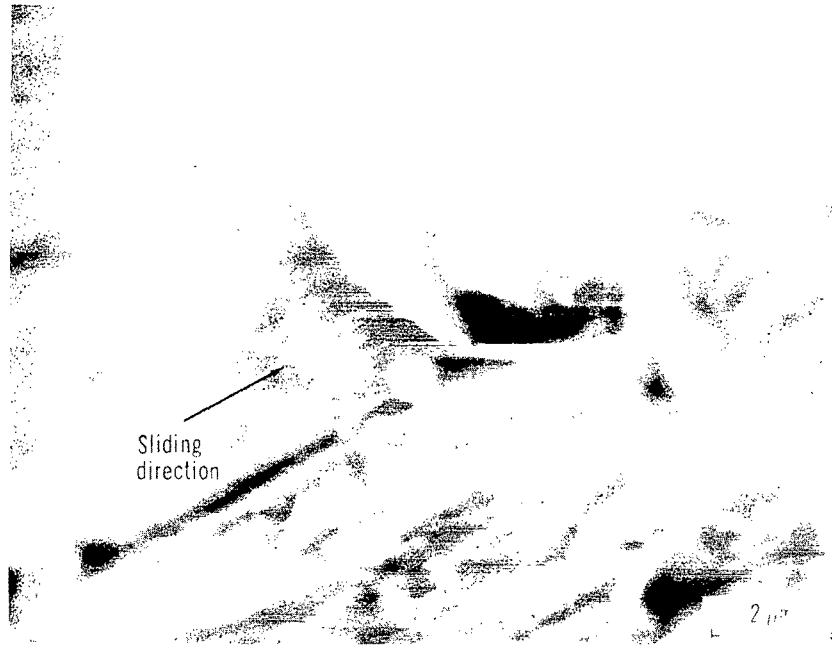

(a) Wear debris.

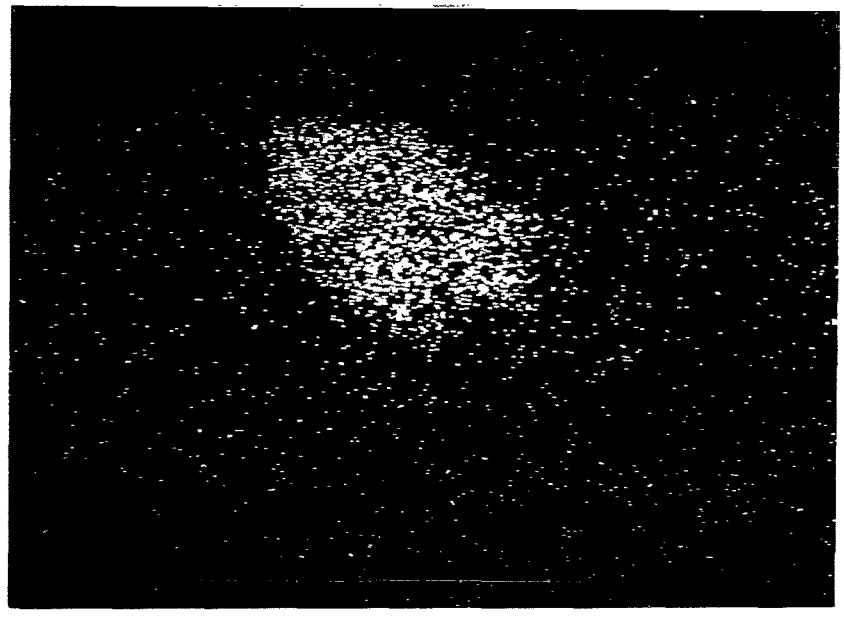

(b) Manganese K_α X-ray map; $4.5X10^3$ counts.

Figure 13. - Scanning electron micrograph and energy dispersive X-ray analysis of wear debris of single-crystal manganese-zinc ferrite transferred to iron rider as result of five passes in high vacuum (10^{-8} N/m^2). Sliding velocity, 3 mm/min; temperature, 25° C.

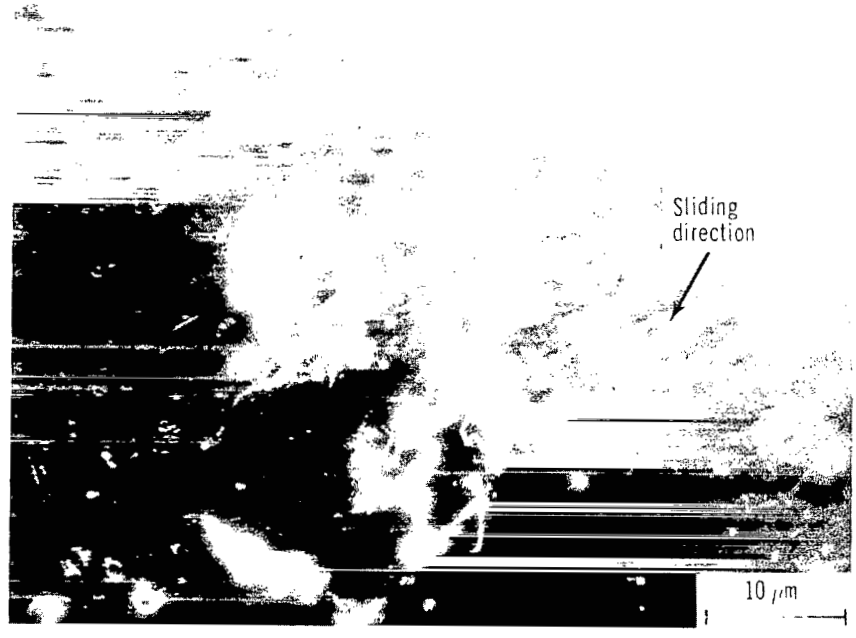

(a) Wear debris

(b) Larger wear debris of SCF.

Figure 14. - Scanning electron micrographs of wear debris of single-crystal manganese-zinc ferrite transferred to titanium rider as result of single pass in high vacuum (10^{-8} N/m^2). Sliding velocity, 3 mm/min; temperature, 25° C.

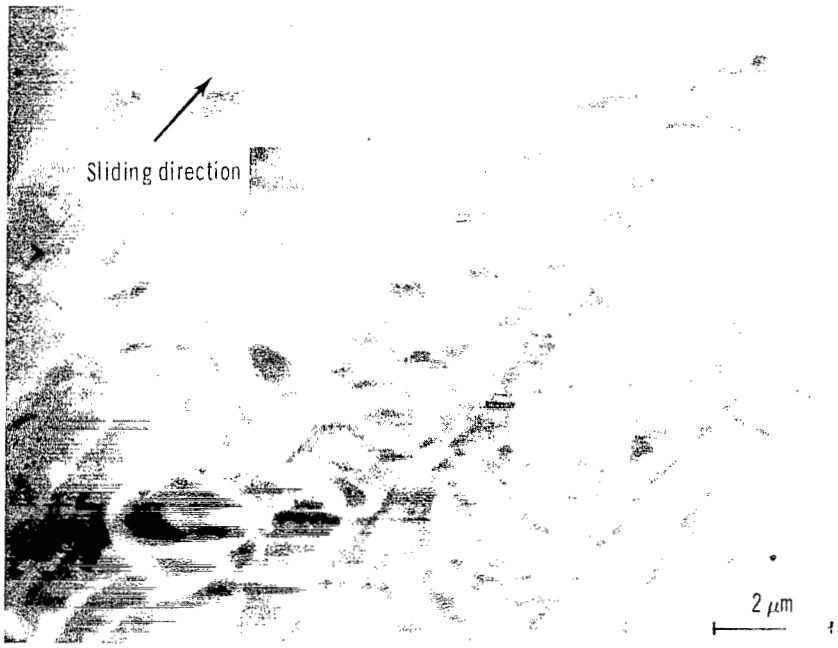

(a) Indentations on rhodium rider produced by rolling of wear debris of HPF as result of single pass.

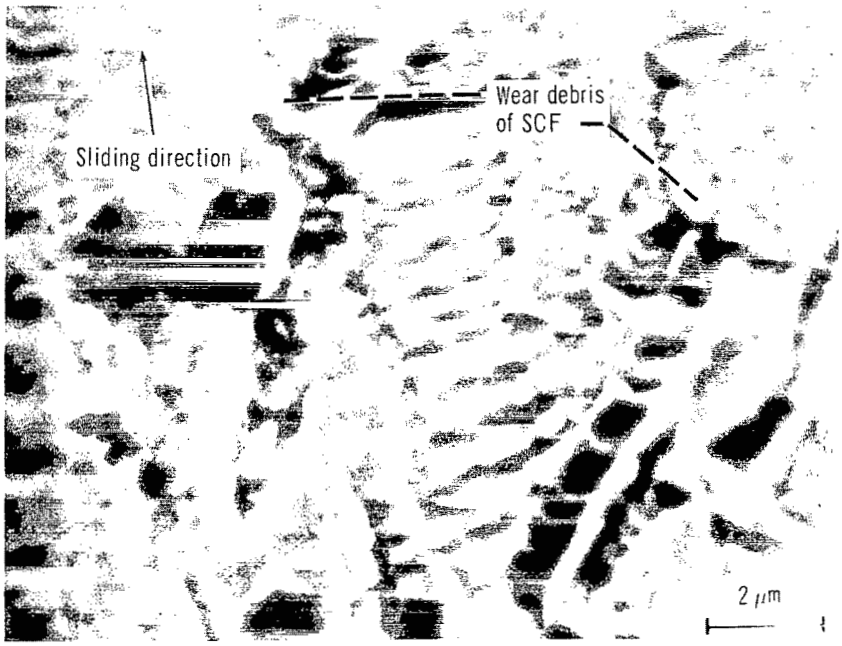

(b) Indentations on cobalt rider produced by rolling of wear debris of SCF as result of single pass.

Figure 15. - Scanning electron micrographs of indentations and grooves on metals and manganese-zinc ferrites after sliding in high vacuum (10^{-8} N/m^2). Sliding velocity, 3 mm/min; load, 30 grams; temperature, 25° C.

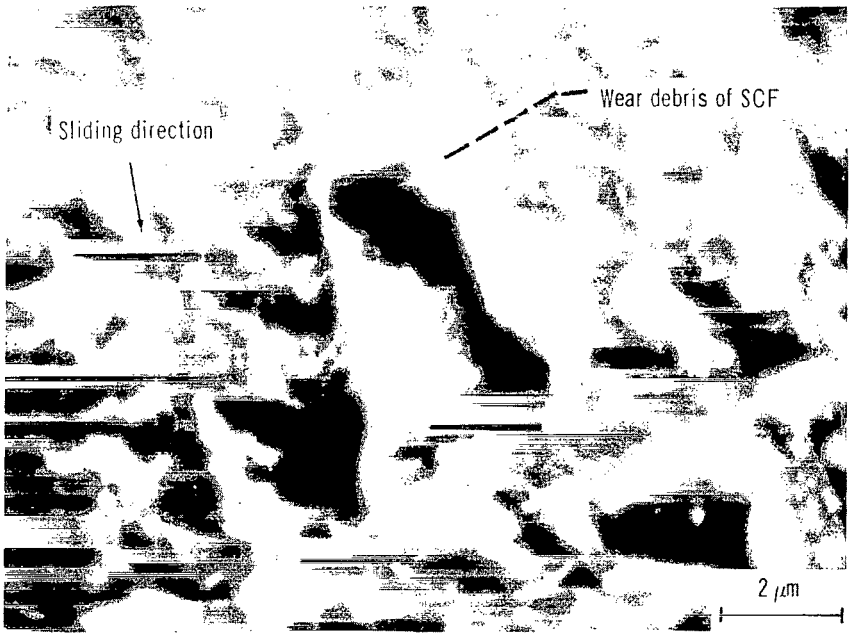

(c) Groove on nickel rider produced by sliding of wear debris of SCF as result of single pass.

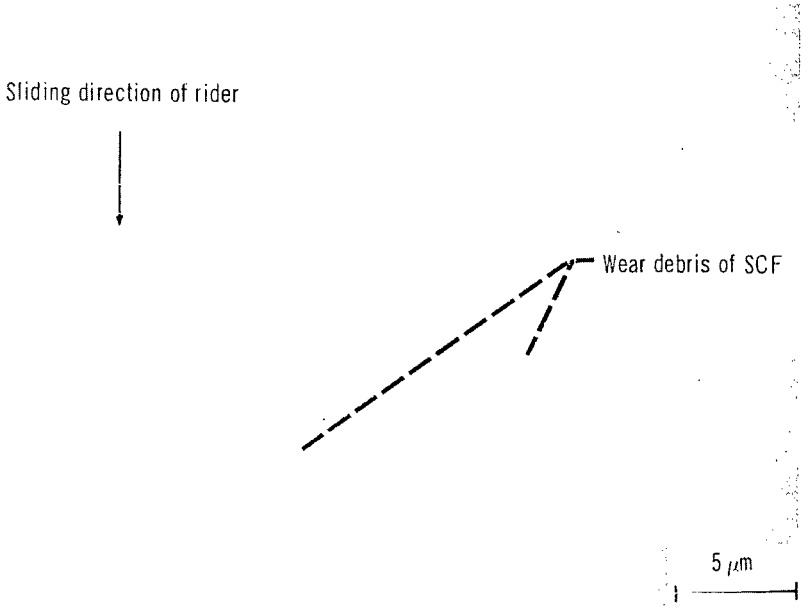

(d) Groove and indentations on SCF produced by sliding and rolling of wear debris of SCF as result of five passes.

Figure 15. - Concluded.

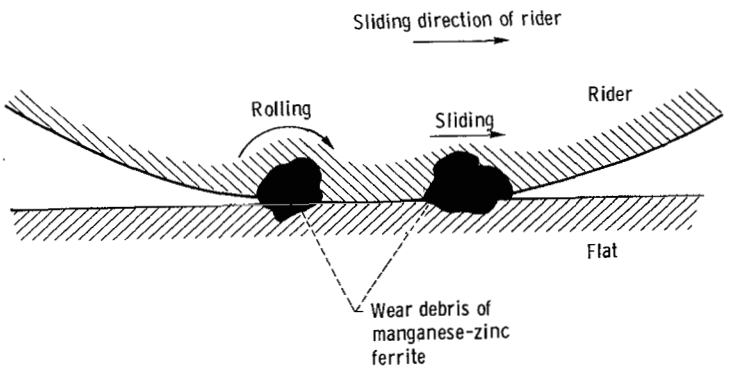

Figure 16. - Rolling and sliding of wear debris.

1. Report No.	2. Government Accession No.	3. Recipient's Catalog No.
NASA TP-1059		

4. Title and Subtitle	5. Report Date
FRICTION AND WEAR OF SINGLE-CRYSTAL AND POLYCRYSTALLINE MANGANESE-ZINC FERRITE IN CONTACT WITH VARIOUS METALS	October 1977
	6. Performing Organization Code
7. Author(s)	8. Performing Organization Report No.
Kazuhisa Miyoshi and Donald H. Buckley	E-9168
	10. Work Unit No.
9. Performing Organization Name and Address	506-16
National Aeronautics and Space Administration Lewis Research Center Cleveland, Ohio 44135	11. Contract or Grant No.
	13. Type of Report and Period Covered
12. Sponsoring Agency Name and Address	Technical Paper
National Aeronautics and Space Administration Washington, D.C. 20546	14. Sponsoring Agency Code

15. Supplementary Notes

16. Abstract

Sliding friction experiments were conducted with single-crystal (SCF) and hot-pressed polycrystalline (HPF) manganese-zinc ferrite in contact with various metals. Results indicate that the coefficients of friction for SCF and HPF are related to the relative chemical activity of those metals in a high vacuum (10^{-8} N/m^2). The more active the metal, the higher the coefficient of friction. The coefficients of friction for both SCF and HPF were the same and much higher in vacuum than in argon at atmospheric pressure. All the metals tested transferred to the surface of both SCF and HPF in sliding. Both SCF and HPF exhibited cracking and fracture with sliding. Cracking in SCF is dependent on crystallographic characteristics. In HPF, cracking depends on the orientation of the individual crystallites.

17. Key Words (Suggested by Author(s))

Single-crystal manganese-zinc ferrite; Polycrystalline manganese-zinc ferrite; Friction; Wear; Chemical activity; Auger

18. Distribution Statement

Unclassified - unlimited
STAR Category 27

19. Security Classif. (of this report)	20. Security Classif. (of this page)	21. No. of Pages	22. Price*
Unclassified	Unclassified	27	A03

* For sale by the National Technical Information Service, Springfield, Virginia 22161

National Aeronautics and
Space Administration

Washington, D.C.
20546

Official Business
Penalty for Private Use, $300

THIRD-CLASS BULK RATE

Postage and Fees Paid
National Aeronautics and
Space Administration
NASA-451

7 1 1U,C, 100777 S00903DS
DEPT OF THE AIR FORCE
AF WEAPONS LABORATORY
ATTN: TECHNICAL LIBRARY (SUL)
KIRTLAND AFB NM 87117

NASA

POSTMASTER: If Undeliverable (Section 158 Postal Manual) Do Not Return